

Galectin-3 Binding Protein and Galectin-1 Interaction in Breast Cancer Cell Aggregation and Metastasis

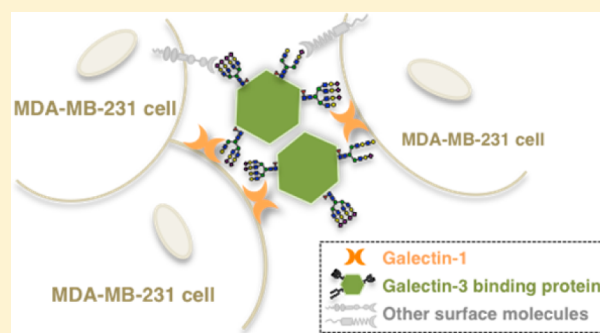
Tzu-Wen Lin,^{†,‡} Hui-Tzu Chang,^{†,§,‡} Chein-Hung Chen,[†] Chung-Hsuan Chen,[†] Sheng-Wei Lin,[‡] Tsui-Ling Hsu,[†] and Chi-Huey Wong^{*,†}

[†]Genomics Research Center and [‡]Institute of Biological Chemistry, Academia Sinica, 128 Academia Road, Section 2, Nankang, Taipei 115, Taiwan

[§]Institute of Biochemistry and Molecular Biology, National Yang-Ming University, Taipei 112, Taiwan

S Supporting Information

ABSTRACT: Galectin-3 binding protein (Gal-3BP) is a large hyperglycosylated protein that acts as a ligand for several galectins through glycan-dependent interactions. Gal-3BP can induce galectin-mediated tumor cell aggregation to increase the survival of cancer cells in the bloodstream during the metastatic process. However, the galectin interacting with Gal-3BP and its binding specificity has not been identified and structurally elucidated, mainly due to the limitation of mass spectrometry in glycan sequencing. To understand the role of Gal-3BP, we here used liquid chromatography–mass spectrometry combined with specific exoglycosidase reactions to determine the sequences of N-glycans on Gal-3BP from MCF-7 and MDA-MB-231 cells, especially the sequences with terminal sialylation and fucosylation, and addition of LacNAc repeat structures. The N-glycans from both strains are complex type with terminal α 2,3-sialidic acid and core fucose linkages, with additional α 1,2- and α 1,3 fucose linkages found in MCF-7 cells. Compared with that from MCF-7, the Gal-3BP from MDA-MB-231 cells had fewer tetra-antennary structures, only α 1,6-linked core fucoses, and more LacNAc repeat structures; the MDA-MB-231 cells had no surface galectin-3 but used surface galectin-1 for interaction with Gal-3BP to form large oligomers and cell aggregates. This study elucidates the specificity of Gal-3BP interacting with galectin-1 and the role of Gal-3BP in cancer cell aggregation and metastasis.



INTRODUCTION

Glycoconjugates on the cell surface play important roles in a variety of biological functions. Various glycan structures are present in different cell types and at different developmental and differentiation stages and are modified in many pathological states including cancers.¹ Aberrant glycosylation is frequently observed in various tumor cells, and some glycan biomarkers have been utilized for detection of cancer (e.g., CA19-9 and CA-125) and development of vaccines.² Glycan changes in glycoproteins that correlate with tumor progression include aberrant branching of N-linked glycans, terminal sialylation and fucosylation, expression of sialylated Lewis structures, truncation of O-linked glycans, and expression of the poly-*N*-acetylglucosamine (poly-LacNAc) structure.³ Altered oligosaccharides on glycoproteins can affect glycoprotein folding and stability and interfere with carbohydrate–carbohydrate, carbohydrate–protein, and glycoprotein–glycoprotein interactions, and as a result, regulate many physiological and pathological events. Therefore, specific glycan structures have been suggested to be signatures of certain disease states such as cancer metastasis.⁴

Gal-3 binding protein (Gal-3BP), also known as Mac-2 binding protein (Mac-2BP) or tumor-associated antigen 90K (TAA90K), is a glycoprotein without a transmembrane domain.

Gal-3BP is expressed in various cell types, including hematopoietic cells and glandular or mucosal epithelia, and is present at high levels in the serum and other biological fluids of patients^{5,6} with pancreatic, breast, or lung cancer and patients with AIDS, hepatitis, and autoimmune diseases.^{7–10} It has been reported that breast cancer patients with serum Gal-3BP exceeding 11 μ g/mL have poor prognosis and metastasis;¹¹ Gal-3BP is therefore considered to be a tumor-associated antigen of breast cancer.

Gal-3BP is a highly glycosylated protein with seven N-linked glycosylation sites. Gal-3BP can self-assemble to form large homo-oligomers in a linear or ring-like shape, and ring–ring association is also observed.¹² These multimeric forms of Gal-3BP are believed to increase the interaction with multiple targets, including galectins-1, -3, and -7, and the extracellular matrix (ECM), including collagen IV, V and VI, fibronectin, laminin-1, -5, and -10, and β 1-integrin). Recently, Gal-3BP was also demonstrated to bind other lectins on immune cells, including dendritic cell-specific intercellular adhesion molecule 3-grabbing nonintegrin (DC-SIGN) and E-selectin,^{13,14} and the interaction of Gal-3BP and Gal-3 has been confirmed to be

Received: May 11, 2015

Published: July 13, 2015

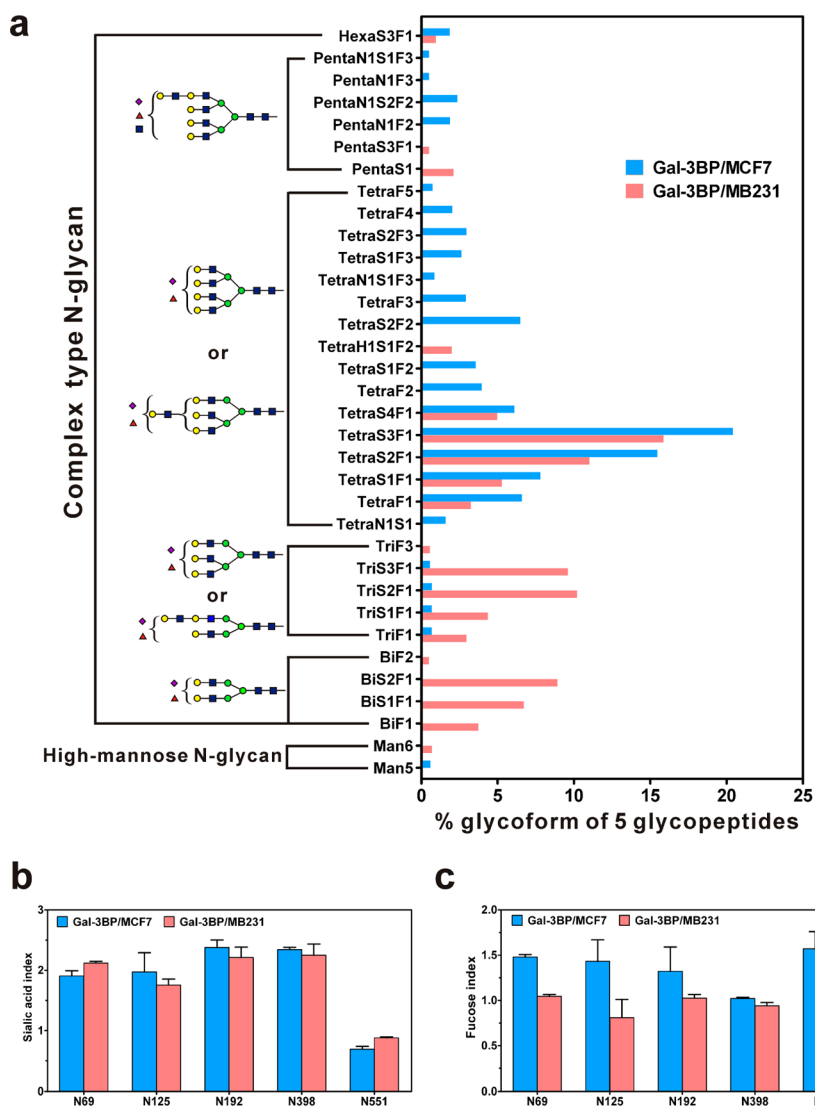


Figure 1. Glycoform profiling of Gal-3BP. (a) Glycoforms of Gal-3BP/MCF7 and Gal-3BP/MB231. (b and c) Site-specific sialylation (b) and fucosylation (c). Sialic acid and fucose indexes were calculated based on the following equation: $\sum(\% \text{ of the glycan with sialic acid/fucose} \times \text{the number of the sialic acid/fucose annotated on the glycan})$. Man, high mannose; Bi/Tri/Tetra/Penta/Hexa, bi/tri/tetra-/penta-/hexa-antennary; F, fucose; S, sialic acid; N,N-acetylhexosamine; H, hexose. Symbols for monosaccharides: fucose, triangle; N-acetylglucosamine, blue square; galactose, yellow circle; mannose, green circle; N-acetylneuraminic acid, diamond.

carbohydrate dependent.^{15,16} Although the biological functions of Gal-3BP remain unclear, the induction of homotypic cell aggregation by Gal-3BP¹⁶ is considered to facilitate tumor metastasis by preventing anoikis of metastatic cells in the bloodstream.¹⁷ Moreover, the interaction of Gal-3BP and ECM may also relate to the adhesiveness of tumor cells *in situ*.¹⁸

As glycosylation plays an important role in modulating the behavior of Gal-3BP in cancer progression, we decided to first identify the galectin that interacts with Gal-3BP and the sequences of N-linked glycans on the Gal-3BP from different breast cancer cell lines to investigate their structures and ability to enhance tumor aggressiveness. The glycan sequences were determined by liquid chromatography–mass spectrometry (LC-MS) combined with exoglycosidase treatment and lectin-based ELISA to overcome the limitation of LC-MS method alone. Gal-3BP from MDA-MB-231, an aggressive breast cancer cell line, induced a higher level of homotypic cell aggregation than the Gal-3BP from MCF-7. We also observed that the Gal-3BP from MDA-MB-231 formed a larger homo-oligomer.

Understanding the differences of Gal-3BPs from MDA-MB-231 and MCF-7 cells in terms of N-glycans sequences and their spatial arrangement as well as the specificity of Gal-3BP-lectin interaction will provide valuable information for use to elucidate the role of Gal-3BP in cancer cell aggregation and metastasis.

RESULTS AND DISCUSSION

It has been proposed that Gal-3BP is a breast cancer-specific antigen.¹⁹ To understand how the glycans on Gal-3BP affect the behavior of breast cancer cells, we overexpressed and purified Gal-3BP in two breast cancer cell lines, MCF-7 (mild) and MDA-MB-231 (aggressive). After PNGaseF digestion to remove the N-linked glycans, the molecular weight of each species shifted from ~90 to 65 kDa as expected (65 331 Da as calculated based its amino acid sequence) (Supporting Information, Figure S1). We then immobilized and compared the Gal-3BPs from MCF-7 and MDA-MB-231 for their binding to Gal-3 in microtiter plates and found that Gal-3 did interact

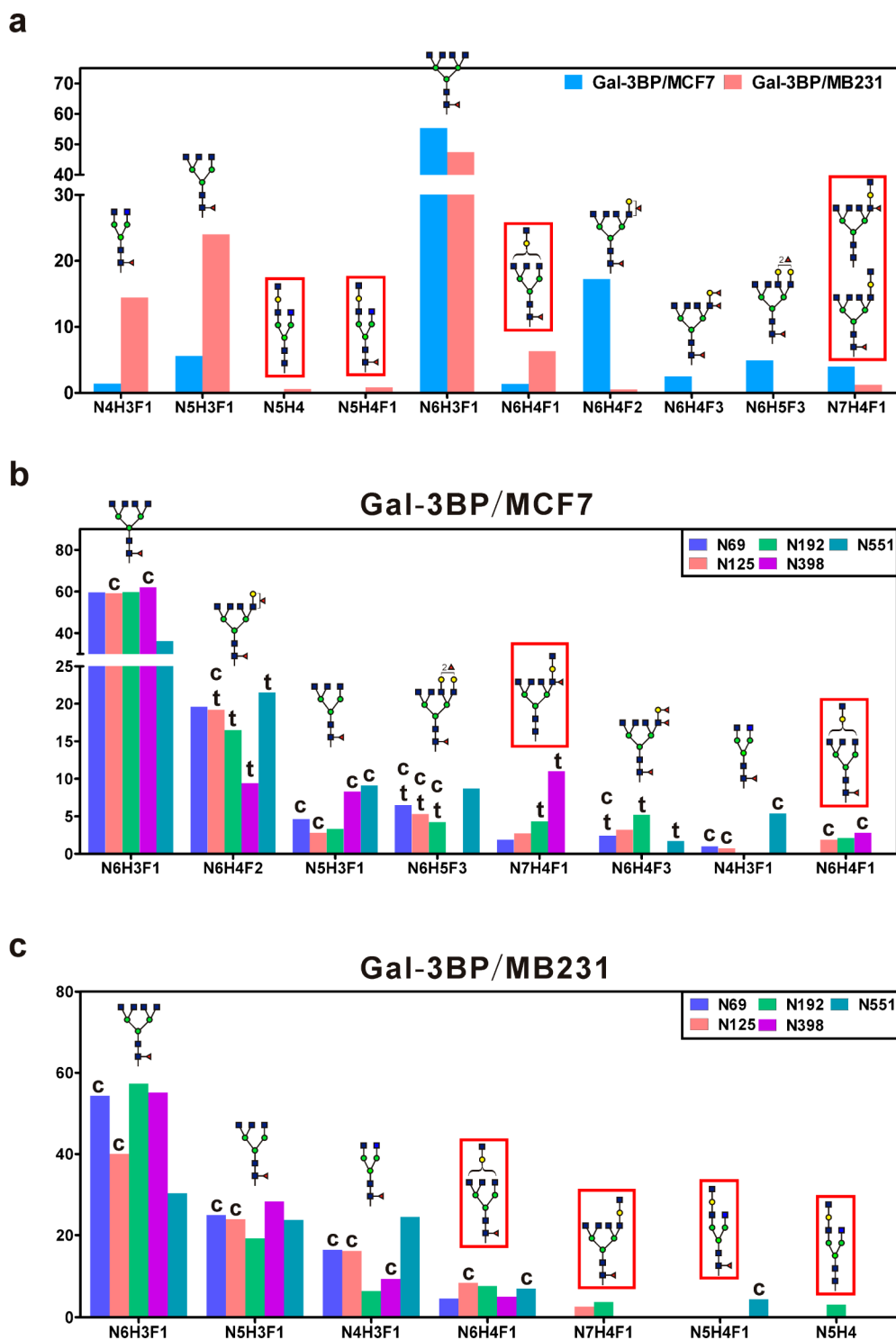


Figure 2. Degalactosylation of Gal-3BP for poly-LacNAc structure determination. (a) Degalactosylated glycoforms of Gal-3BP/MCF7 and Gal-3BP/MB231. (b and c) Site-specific glycoforms of Gal-3BP/MCF7 (b) and Gal-3BP/MB231(c). Possible glycan structures are drawn on top of each bar. The glycoforms with oxonium ions, $m/z = 512.2$, in MS/MS spectra, are labeled with t (terminal fucose). The glycoforms with ions corresponding to the mass of peptide-HexNAc-Fuc fragments in the MS/MS spectra are labeled with c (core fucose). The glycoforms with poly-LacNAc structure are highlighted with red boxes.

with Gal-3BP (Figure S2a). The binding affinity of Gal-3BP/MB231 was significantly higher than Gal-3BP/MCF7 at low concentrations of Gal-3, and a similar trend was also observed in the binding of endogenous Gal-3BP from MCF-7 and MDA-MB-231 toward Gal-3, indicating that the overexpressed Flag-tagged Gal-3BP could represent native Gal-3BP (Figure S2b).

This result suggested that Gal-3BP/MB231 with higher affinity for Gal-3 was due to the N-glycans on Gal-3BPs, since the recombinant Gal-3BP was produced by the same expression construct, and the nucleotide sequences of endogenous Gal-3BP in both MCF-7 and MDA-MB-231 were identical (data not shown).

In order to link the glycans specifically expressed on Gal-3BP of breast cancer cells with their function, we next performed site-specific glycoproteomics of Gal-3BPs by LC-MS/MS. This method is based on matching the experimental masses with the predicted masses of tryptic peptide fragments and the glycans from the CFG carbohydrate database and confirmed the existence of ionized glycan fragments in MS/MS spectra. The glycoforms of individual glycopeptides were quantified and calculated for their proportions in all the glycoforms observed on a specific glycopeptide. Gal-3BP was observed to have N-glycans on the expected glycosylation sites, but there was no O-glycans detected. Five out of seven expected N-glycosylation sites were consistently identified in tryptic glycopeptides, including Asn (N) 69, N125, N192, N398, and N551 (Figure 1a). The other two glycopeptides with N362 and N580, respectively, were detected with very weak signal and therefore were not listed. Most N-linked glycans of Gal-3BPs from these two cell lines were complex-type glycans containing sialic acids and fucoses. High-mannose or hybrid-type glycans were only found at low percentages in the glycopeptide of N551. The size of complex-type glycans and the fucosylation status were very different in Gal-3BP/MCF7 and Gal-3BP/MB231: bigger N-linked glycans were observed in Gal-3BP/MCF7 (MCF7, tetra-antennary 85%; MB231, biantennary 20%, triantennary 28%, and tetra-antennary 43%). The level of sialylation and fucosylation at each glycosylation site was calculated as sialic and fucose indexes (Figure 1b,c) and compared. The results indicated that the levels of sialylation on these two Gal-3BPs were similar, with a lower sialylation on N551. However, the N-linked glycans in Gal-3BP/MB231 had fewer branches and therefore fewer terminal galactoses compared to Gal-3BP/MCF7. There was more fucosylation in Gal-3BP/MCF7, and most N-linked glycans (~90%) on Gal-3BP/MB231 carried only one fucose. Among these five glycosylation sites, N398 was less fucosylated and more sialylated, and N551 was less sialylated and more fucosylated, reflecting a pattern of site-specific glycosylation on Gal-3BP. The glycoform data from MS analysis were consistent with lectin-based ELISA. Six lectins were used to detect the binding with Gal-3BPs (Figure S3): Gal-3BP/MCF7 showed higher PHA-L (for tri- or tetra-antennary N-linked glycans) and UEA-I (for α 1,2-linked fucose) binding intensities, and Gal-3BP/MB231 showed higher MAL-II, SNA, and LEL binding intensities. Therefore, the glycoforms of Gal-3BP/MCF7 contained more tri- or tetra-antennary N-linked glycans and α 1,2-linked fucoses, while Gal-3BP/MB231 had smaller N-linked glycans and had more poly-LacNAc structures.

Poly-LacNAc is a high-affinity ligand for Gal-3. In the lectin assay, we discovered that Gal-3BP could be recognized by LEL, which binds to poly-LacNAc. The number of poly-LacNAc moieties on Gal-3BP may be an important key factor affecting the affinity for Gal-3. Here, we have designed a method to identify poly-LacNAc on Gal-3BP glycopeptides using β 1,3/4-galactosidase to differentiate from the multibranching LacNAc structures. Before enzyme digestion, we chemically removed the terminal sialic acid to expose terminal galactose residues and then used β 1,3/4-galactosidase to remove the terminal galactose. If the N-glycans contain poly-LacNAc residues, the outer galactose is removed by the enzyme, but the exposed GlcNAc can protect the inner galactose from further cleavage. The terminal fucoses, including the α 1,2-, α 1,3-, or α 1,4-fucose linkages also resist β 1,3/4-galactosidase digestion. In addition, we checked the MS/MS spectrum to detect the presence of

512.2 oxonium ion as an indicator of the terminal fucose signal and peptide+HexNAc+Fuc ion as a core fucose signal (Table S1). The results showed that major N-glycans with one fucose have no 512.2 oxonium ion signal, indicating core fucosylation. Therefore, the N-glycans with extra hexose residues (over three core mannoses) without outer fucose residues could be derived from the N-glycans containing the poly-LacNAc substructure. Degalactosylated glycopeptides were analyzed using LC-MS/MS to observe glycan compositions (Figure 2) and the location of fucose. Only four glycoforms, N5H4S0F0, N5H4S0F1, N6H4S0F1, and N7H4S0F1 corresponded to the N-glycans with poly-LacNAc.

We calculated the sum of these four glycoforms in every N-glycosite on the Gal-3BPs (Table 1). Gal-3BP/MB231 had

Table 1. Potential N-Glycans with Poly-LacNAc in the N-Glycosylation Site

N-glycosite	Gal-3BP from MCF-7	Gal-3BP from MDA-MB-231
N69	1.94%	4.40%
N125	4.58%	10.75%
N192	6.42%	14.43%
N398	13.76%	4.81%
N551	0.00%	11.07%
average	5.34%	9.01%

higher glycoforms with poly-LacNAc (9.01%) than MCF-7 (5.34%). Furthermore, the distribution of N-glycans with poly-LacNAc on the glycosites was different in these two Gal-3BPs; Gal-3BP/MB231 had three glycosites (N125, 192 and 551) over 10%, but Gal-3BP/MCF7 had only one (N398), and the major glycoform on Gal-3BP/MB231 was from N6H4S0F1 and that on Gal-3BP/MCF7 was from N7H4S0F1. This result indicated that the higher binding ability of Gal-3BP/MB231 for Gal-3 could come from the contribution of the poly-LacNAc substructure.

Through degalactosylated glycopeptide profiling, we also discovered and determined the major glycoforms of Gal-3BP/MCF7 (Figure 2b) and Gal-3BP/MB231 (Figure 2c). After galactosidase digestion, most N-glycans of Gal-3BP/MB231 only retained three hexose residues from the core structure and had only one fucose. Based on the characteristics of enzyme digestion and MS/MS spectra of glycopeptides, we believe that the location of the fucose residue was on the N-glycan core (core fucosylation). On the other hand, there was almost no terminal fucose signal in the MS/MS spectra of Gal-3BP/MB231 glycopeptides. Therefore, the three major glycoforms of Gal-3BP/MB231 were bi- (14.5%), tri- (24%), and tetra-antennary (47.4%) N-glycans with a core fucose and several sialic acids. The major degalactosylated glycoform of Gal-3BP/MCF7 was N6H3S0F1 (~50%) derived from a tetra-antennary N-glycan with core fucose. The other glycoforms also had six HexNAc residues and multiple fucose residues, so we concluded that the major glycoform of Gal-3BP/MCF7 was the tetra-antennary structure with a core fucose and outer arm fucose and sialic acids. These results were also confirmed by the glycopeptide profiling and lectin assay.

The other specific exoglycosidases, including α 2,3-sialidase and α 1,2- and α 1,3/4-fucosidase, are useful for determining the terminal sialic acid and fucose linkages, which are difficult to obtain using mass spectra only. We also compared the glycopeptide profiling of Gal-3BP before and after exoglycosidase digestion. First, we used α 2,3-sialidase to remove the α 2,3-

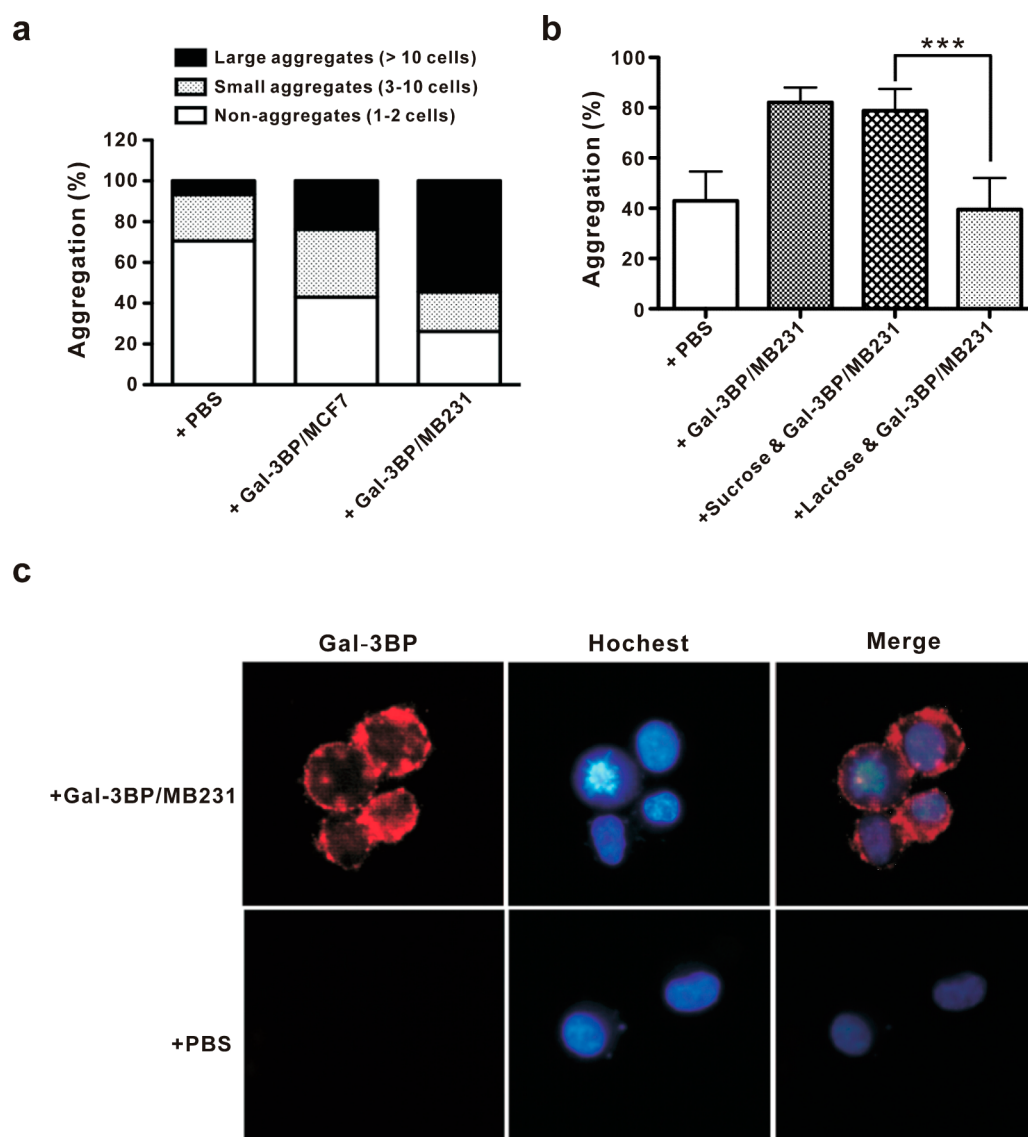


Figure 3. Gal-3BP induced carbohydrate-dependent cell aggregation in breast cancer cells. (a) Induction of MDA-MB-231 aggregation by Gal-3BP/MCF7 or Gal-3BP/MB231. Gal-3BP (5 $\mu\text{g}/\text{mL}$) was used to treat cells for 1 h, and the degree of cell aggregation was quantitated by ImageJ. (b) Homotypic MDA-MB-231 aggregation was inhibited by lactose. Lactose (10 mM) or sucrose (10 mM) was added together with Gal-3BP and degrees of cell aggregation were quantified. Results are shown as mean \pm SD ($n = 5$). ***, $P < 0.001$ compared with sucrose treatment by Student t test. (c) Gal-3BP was detected on the cell surface and at the regions of cell–cell contact under fluorescence microscopy. MDA-MB-231 cells were subjected to aggregation assay and then stained with anti-Gal-3BP pAb (red) or Hoechst 33342 (nuclear stain, shown in blue color). The cells incubated with PBS were stained as a negative control.

linkage sialic acid specifically from the tryptic Gal-3BP glycopeptides (Figure S4a). The result showed that most sialic acid (over 95%) was removed by this enzyme, indicating that the major sialylation in these two Gal-3BPs was the $\alpha 2,3$ -linkage. Second, $\alpha 1,2$ - and $\alpha 1,3/4$ -fucosidase can release terminal $\alpha 1,2$ -fucose and subterminal $\alpha 1,3/4$ -fucose, respectively. Before the treatment with these two enzymes, we also removed the terminal sialic acid to simplify the glycoforms and improve signal intensity. According to the previous result, the N-glycans on Gal-3BP/MB231 usually carry only one fucose, and the fucose is located in the inner N-glycan (core fucose) and is not removed by these two fucosidases. Gal-3BP/MCF7 has many multiple fucosylated glycoforms and was thus performed using fucosidase digestion (Figure S4b). After $\alpha 1,2$ -fucosidase treatment, we observed a small increase in monofucosylated N-glycans and a decrease in N-glycans with

2–5 fucose residues. In addition, this digestion only occurred at the N69, 125, and 192 sites with the fucosylation level at the N398 and N551 sites remaining unchanged. The other fucosidase, $\alpha 1,3/4$ -fucosidase, could reduce the size of N-glycans by 2–5 fucoses to about 50% at every N-glycosylation site. Therefore, $\alpha 1,2$ -fucosylation in Gal-3BP/MCF7 is less than $\alpha 1,3$ -fucosylation but is site-specific. These two fucosidases cannot remove all fucose residues in the N-glycans (as the N-glycans without fucose did not increase), and this result also indicates that most N-glycans in MCF-7 cells have a core fucose.

In summary, the N-glycans of Gal-3BP/MCF7 were tetraantennary N-glycans with terminal $\alpha 2,3$ -sialic acids and terminal fucoses and about 5% contained the poly-LacNAc substructure. The N-glycans of Gal-3BP/MB231 contained mixtures of bi-, tri-, and tetra-antennary N-glycans with 2–3

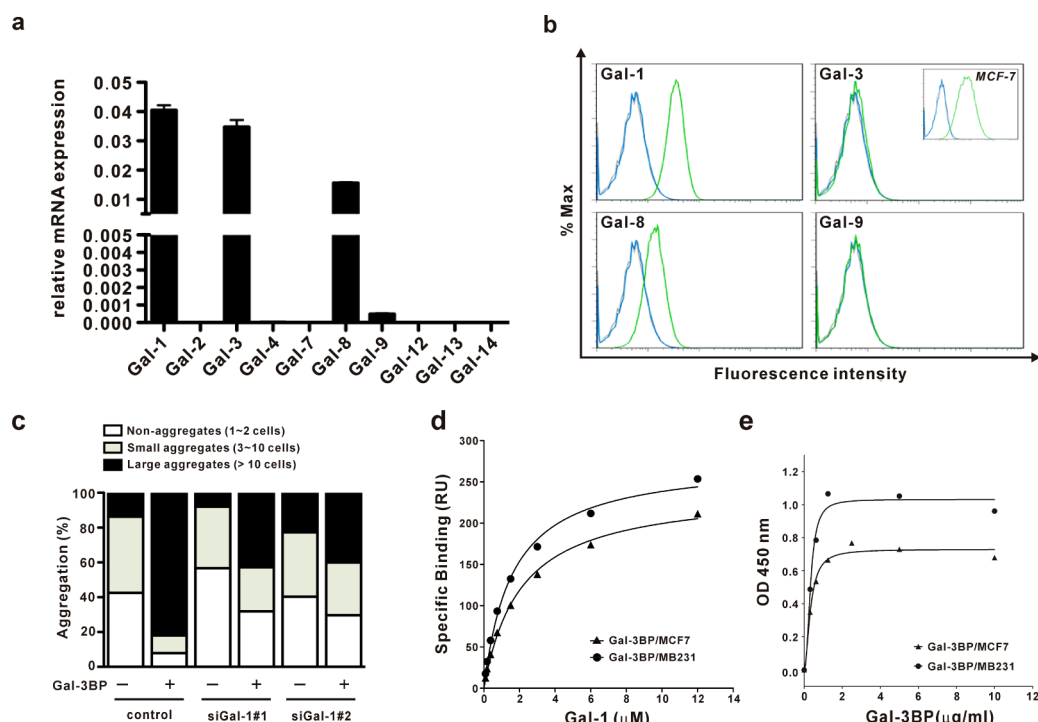


Figure 4. Expression profiles of galectin (Gal) in breast cancer MDA-MB-231 cells and the interaction of Gal-1 and Gal-3BP. (a) Q-PCR analysis for Gal mRNA expression in MDA-MB-231 cells. The expression of Gal was normalized against the expression level of GAPDH mRNA. (b) Flow-cytometric analysis of galectin expression on MDA-MB-231 cells. Blue histograms, isotype control staining; green histograms, anti-galectin staining. Inset: Flow-cytometric analysis of Gal-3 expression on MCF-7 cells. (c) Aggregation of the cells knocked down with Gal-1 upon treatment of Gal-3BP. MDA-MB-231 cells transfected with negative control or Gal-1 siRNA were incubated in the presence of Gal-3BP/MB231 (10 μg/mL). After 1 h of incubation, the degrees of cell aggregation were quantitated by ImageJ. (d) SPR-derived steady-state affinity for Gal-1 and Gal-3BP interactions. Gal-3BP/MCF7 and Gal-3BP/MB231 were immobilized on sensor chips, and Gal-1 in various concentrations was applied to calculate the K_D values. (e) Binding ability of Gal-3BPs to immobilized Gal-1 in the ELISA assay.

terminal $\alpha 2,3$ -sialic acids and a core fucose, and about 9% of the glycans contained the poly-LacNAc substructure.

Gal-3BP functions in the induction of homotypic cell aggregation, and the mechanism is considered to proceed through Gal-mediated carbohydrate-dependent interaction. In previous studies, Gal-3BPs showed different binding affinities for Gal-3. We therefore performed the cell aggregation assay to compare the activity (Figure 3). Compared to Gal-3BP/MCF7, Gal-3BP/MB231 could induce more aggregates of MDA-MB-231 cells. Moreover, we also observed that the ratio of larger aggregates (over 10 cells) induced by Gal-3BP/MB231 was obviously higher than that of Gal-3BP/MCF7. In the microscopic images, huge cell aggregates were observed after treatment with Gal-3BP, and the added Gal-3BP was found to be located at the cell–cell contact region as shown by the anti-Gal-3BP antibody staining (Figure 3c). Because the aggregation of MDA-MB-231 cells induced by Gal-3BP was also inhibited by lactose but not sucrose (Figure 3b), it is believed to be a carbohydrate-dependent interaction.

In order to understand whether MDA-MB-231 cell aggregation was galectin dependent, we investigated the expression profiles of all the known human Gals in MDA-MB-231 cells. By examining the mRNA expression via Q-PCR and their expression levels on the cell surface by flow cytometry (Figure 4), we found that MDA-MB-231 cells could express Gal-1, -3, -8, and -9 mRNA. However, it is interesting that only Gal-1 and -8, but not Gal-3, were detected on the cell surface of MDA-MB-231 (Figure 4b), while the expression of Gal-3 was detected on MCF-7 (Figure 4b, inset of Gal-3 staining),

indicating that anti-Gal-3 could detect Gal-3 on the cell surface. This result suggested that the aggregation of MDA-MB-231 induced by Gal-3BP was not mediated by Gal-3 and could possibly be mediated by Gal-1 or -8. Interaction of Gal-1 and Gal-3BP was reported to be involved in homotypic cell aggregation in human melanoma A375 cell line. To explore the relative contribution of Gal-1 to MDA-MB-231 cell aggregation, Gal-1-deficient cells were established by two kinds of Gal-1 siRNA (siGal1#1 and siGal1#2). The mRNA and cell surface expressions of Gal-1 in the two Gal-1-deficient cell lines were significantly reduced compared to parental and control cells (Figure S5). We performed cell aggregation assay with or without additional Gal-3BP (Figure 4c). Gal-1-deficient cells had less cell aggregation induced by Gal-3BP, and the percentage of large aggregates (siGal1#1:43%, siGal1#2:40%) was lower compared to control cells. This result suggested that Gal-3BPs interact with Gal-1 on the cell surface to induce MDA-MB-231 cell aggregation with large cell aggregates. To analyze the interaction between Gal-1 and Gal-3BPs, we performed surface plasmon resonance (SPR). The sensorgrams revealed that the association and dissociation of Gal-1 to Gal-3BPs was very rapid (Figure S6). The K_D values of Gal-3BP/MCF7 and Gal-3BP/MB231 binding to Gal-1 calculated by steady-state analysis were 2.34 and 1.88 μM, respectively, showing that the binding affinity of Gal-1 for Gal-3BP/MCF7 is slightly higher (Figure 4d). Interestingly, the binding of Gal-3BP/MCF7 and Gal-3BP/MB231 to immobilized Gal-1 in the ELISA experiment also showed that Gal-3BP/MB231 had a

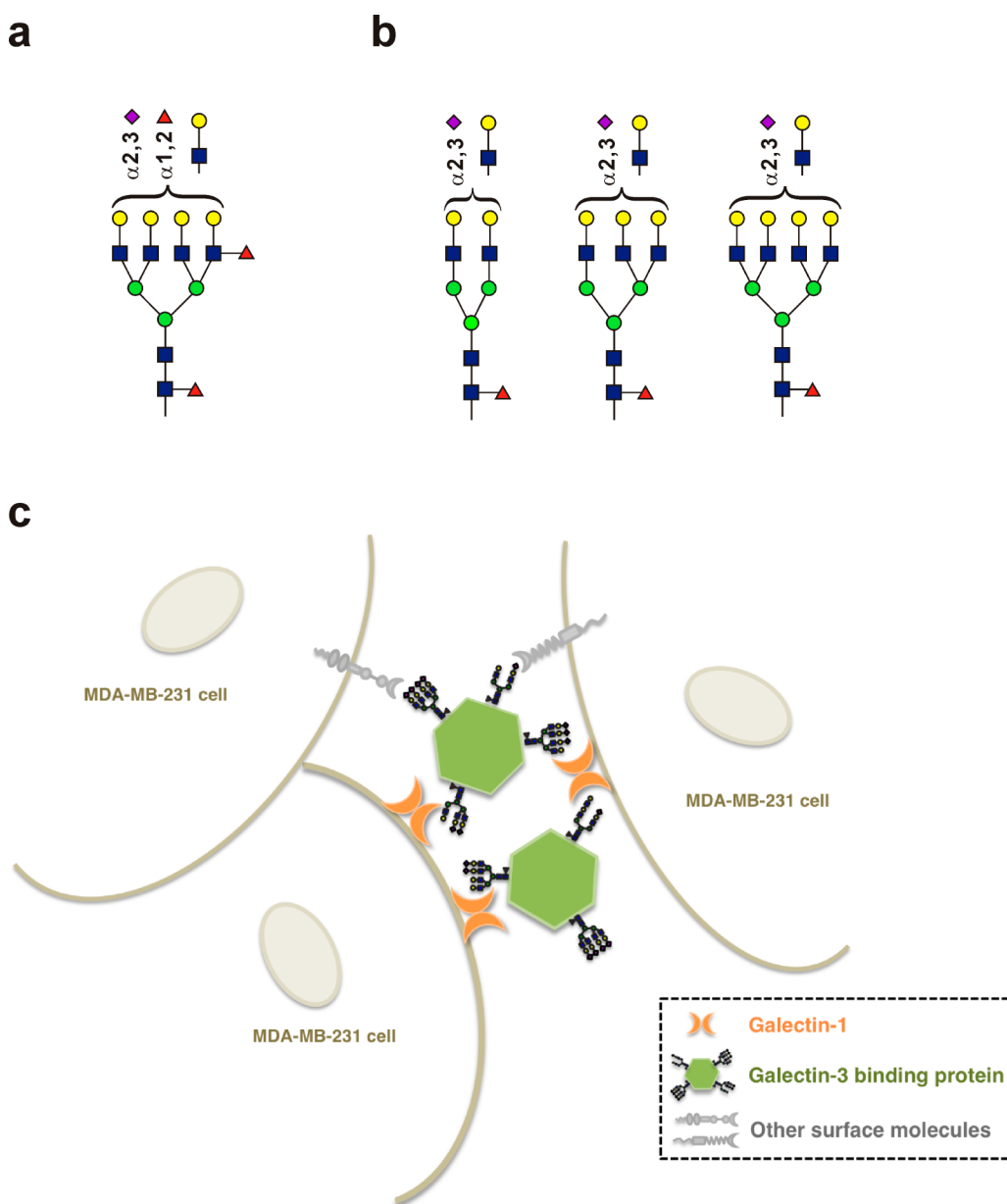


Figure 5. Major glycoforms of Gal-3BP derived from MCF-7 cells (A) and MDA-MB-231 cells (B), and a hypothesized model of Gal-3BP-induced cell aggregation (C).

higher binding affinity toward Gal-1 comparing to Gal-3BP/MCF7 (Figure 4e).

Because of oligomerization, native human Gal-3BPs can self-assemble to form huge macromolecules with ring-like structures. These protein macromolecules contain 10–16 monomers and about 70–116 N-glycans on one protein oligomer. A previous study indicated that Gal-3BP oligomers may contribute to the multivalent effect of Gal-3BP, which binds to multiple targets.¹⁵ To validate the oligomerization of the Gal-3BPs, we observed protein oligomers of Gal-3BP/MCF7 and Gal-3BP/MB231 using HPLC SEC-MALLS (Figure S7). Analysis of the molar mass of these two protein oligomers indicated that Gal-3BP/MB231 could form bigger oligomers (1502 kDa) than Gal-3BP/MCF7 (1138 kDa). Based on the molecular weight of Gal-3BP monomer (~90 kDa), Gal-3BP/MB231 oligomer is composed of 16–17

monomers, and Gal-3BP/MCF7 oligomer is composed of 12–13 monomers.

In this study, we investigated the glycosylation changes in breast cancer cells to understand why the tumor cells show altered glycosylation state during tumorigenesis. We studied the glycosylation profile of a hyperglycosylated glycoprotein, Gal-3BP, which has been suggested to be a breast cancer marker, from two cell lines (MCF-7 and MDA-MB-231) with different metastatic abilities. We used LC-MS/MS to analyze the glycoforms of Gal-3BP glycopeptides site-specifically and introduced exoglycosidases with linkage specificity to facilitate the determination of detailed glycan structures, including the linkages of terminal sialic acids and fucoses, and the substructures of glycan branching and poly-LacNAc.

The results revealed that Gal-3BP/MB231 had a stronger interaction with Gal-3 than Gal-3BP/MCF7 (Figure S2) did. Since Gal-3BP interacts with Gal-3 in a carbohydrate-

dependent manner, the glycans on Gal-3BP are the major factors that modulate the interaction with Gal-3. It has been reported that a tetraantennary N-linked glycan fully capped with sialic acid can also interact with Gal-3, and the binding intensity can be increased up to 8-fold if one poly-LacNAc unit is added.²⁰ Our glycan profiling results showed that poly-LacNAc was more predominant on Gal-3BP/MB231, indicating that this structure could be the key determinant in binding to Gal-3. Glycan profiling showed that the major glycoforms of Gal-3BPs from both breast cancer cell lines were bi-, tri-, and tetra-antennary N-linked glycans with sialylation and fucosylation. It has been reported that α 2,3- and α 2,6-sialylation and α 1,3-fucosylation can partially or completely inhibit the binding between Gal-3BP and Gal-3, while α 1,2-fucosylation has no inhibitory effect on Gal-3BP/Gal-3 interaction.²¹ This finding is also supported by our results that showed that removal of the sialic acids on Gal-3BP increased its binding ability to Gal-3 (data not shown).

We also determined the position of fucose by LC-MS/MS. The oxonium ion with $m/z = 512.2$ (Hex-HexNAc-Fuc) can be used to identify terminal fucosylation. The profile of glycoforms after exogalactosidase treatment also helps locate terminal fucoses since the enzyme is unable to cleave terminal galactose if the LacNAc unit is fucosylated. However, if the position of the fucose cannot be clearly assigned, especially when there is only one fucose in the whole glycan, it is difficult to locate the position of LacNAc unit in the poly-LacNAc structure or as a branch of the glycan chain. In this case, treatment with β 1,3/4-galactosidase plus α 1,2- and β 1,3/4-fucosidases can be used to assign the correct glycan structures.

In order to understand the effect of N-glycans on Gal-3BPs, we performed an aggregation assay by treating MDA-MB-231 cells with Gal-3BPs. Our result was consistent with reports that the formation of Gal-3BP-induced cell aggregates is a carbohydrate-dependent process, because the aggregation was suppressed in the presence of lactose (Figure 3b). Aggregation of cancer cells can facilitate metastasis by preventing anoikis of cells, a kind of apoptosis induced by loss of cell anchorage. The imaging data also showed that Gal-3BP/MB231 induced more and larger cell aggregates than Gal-3BP/MCF7. In addition to enabling the survival of metastatic cells through anoikis, large cell aggregates also promote cell extravasation when getting to the metastasized sites.²² Our data suggest that Gal-3BP may influence the behavior of cells through its glycosylation, which contributes to the metastasis of cancer cells.

It is also important to determine the galectins involved in the MDA-MB-231 cell aggregation. We stained the Gal-1, -3, -8, and -9 on the cell surface using flow cytometry (Figure 4b), and the results indicated that Gal-3 was not expressed on the surface of MDA-MB-231 cells. Knockdown of Gal-1 was found to inhibit the formation of large cell aggregates in MDA-MB-231 cells, indicating that the behavior of Gal-3BP-induced cell aggregation can be mediated by Gal-1.

It has been reported that in N-linked glycans, poly-LacNAc is added by β -1,3-N-acetylglucosaminyltransferase (β 3GNT) and β -1,4-galactosyltransferase (β 4GalT),²³ after the branching process catalyzed by β -1,6-N-acetylglucosaminyltransferase V (GNT-V, encoded by *Mgat5*), and both GNT-V overexpression and poly-LacNAc structure are highly associated with cancer metastasis.^{24–26} The interaction of Gal-3 to poly-LacNAc is thought to be involved in tumorigenic process.²⁷ Although Gal-1 and Gal-3 can interact with poly-LacNAc, Gal-1 prefers to bind terminal LacNAc residue,²⁸ and Gal-3 prefers to internal

LacNAc.²¹ Terminal α 2,3-sialylation or α 1,2-fucosylation of poly-LacNAc was found to have no significant effect on Gal-1 or Gal-3 recognition of poly-LacNAc, while α 1,3/4-fucosylation blocks Gal-1 and Gal-3 binding.^{21,29} In our study, we investigated extensively the N-glycan structures including sialylation, fucosylation, and poly-LacNAc. Our results showed that the Gal-3BP expressed in more aggressive breast cancer cells MDA-MB-231 contained more poly-LacNAc structures and less subterminal α 1,3/4-fucosylation compared to the Gal-3BP from MCF-7. Therefore, the Gal-3BP derived from MDA-MB-231 has better binding ability to Gal-1 on cell surface and induces a higher level of cell aggregation.

Gal-3BP can self-assemble to form large oligomers, and according to the results from SEC-MALLS analysis (Figure S7), Gal-3BP/MB231 formed larger oligomers (16–17 monomers) than Gal-3BP/MCF7 (12–13 monomers). In cell aggregation assay, we also observed that Gal-3BP/MB231 could induce larger cell aggregates, perhaps due to the interaction with cell surface Gal-1 to provide a higher degree of multivalent interaction between cells.

In conclusion, we analyzed the detailed glycoforms of Gal-3BP/MCF7 and Gal-3BP/MB231 using LC-MS/MS and exoglycosidase treatment and compared the differences in the N-linked glycan structures, including terminal sialylation, fucosylation, branching, and poly-LacNAc. The profiles of site-specific glycoforms of the proteins provide some information regarding their spatial orientation in modulating protein function and multivalent interaction (Figure 5). We further demonstrated that changes in Gal-3BP glycosylation can affect the binding for Gal-3 and Gal-1, the ability of Gal-3BP-mediated cell aggregation, and protein oligomerization, which can contribute to the metastatic potential of cancer.

■ ASSOCIATED CONTENT

📄 Supporting Information

Supplementary data and experimental procedures. The Supporting Information is available free of charge on the ACS Publications website at DOI: 10.1021/jacs.5b04744.

■ AUTHOR INFORMATION

✉ Corresponding Author

*chwong@gate.sinica.edu.tw

✍ Author Contributions

[†]These authors contributed equally.

📄 Notes

The authors declare no competing financial interest.

■ ACKNOWLEDGMENTS

We thank Dr. Fu-Tong Liu and Dr. Huan-Yuan Chen for providing various materials for galectin-related experiments and helpful discussion, Dr. Hsin-Yung Yen and Ms. Yu-Ling Chang for SEC-MALLS experiments, and the Academia Sinica Genomics Research Center MS Core Facilities for glycan analysis. This research was supported by the Genomics Research Center, Academia Sinica, Taiwan.

■ REFERENCES

- (1) Cazet, A.; Julien, S.; Bobowski, M.; Burchell, J.; Delannoy, P. *Breast Cancer Res.* **2010**, *12*, 204.
- (2) Huang, Y. L.; Hung, J. T.; Cheung, S. K.; Lee, H. Y.; Chu, K. C.; Li, S. T.; Lin, Y. C.; Ren, C. T.; Cheng, T. J.; Hsu, T. L.; Yu, A. L.; Wu, C. Y.; Wong, C. H. *Proc. Natl. Acad. Sci. U. S. A.* **2013**, *110*, 2517.

- (3) Varki, A.; Kannagi, R.; Toole, B. P. In *Essentials of Glycobiology*; Varki, A., Cummings, R. D., Esko, J. D., Freeze, H. H., Stanley, P., Bertozzi, C. R., Hart, G. W., Etzler, M. E., Eds.; Cold Spring Harbor NY: La Jolla, CA, 2009.
- (4) Zhao, Y. Y.; Takahashi, M.; Gu, J. G.; Miyoshi, E.; Matsumoto, A.; Kitazume, S.; Taniguchi, N. *Cancer Sci.* **2008**, *99*, 1304.
- (5) Bair, E. L.; Nagle, R. B.; Ulmer, T. A.; Laferte, S.; Bowden, G. T. *Prostate* **2006**, *66*, 283.
- (6) Grassadonia, A.; Tinari, N.; Iurisci, I.; Piccolo, E.; Cumashi, A.; Innominato, P.; D'Egidio, M.; Natoli, C.; Piantelli, M.; Iacobelli, S. *Glycoconjugate J.* **2002**, *19*, 551.
- (7) Ozaki, Y.; Kontani, K.; Hanaoka, J.; Chano, T.; Teramoto, K.; Tezuka, N.; Sawai, S.; Fujino, S.; Yoshiki, T.; Okabe, H.; Ohkubo, I. *Cancer* **2002**, *95*, 1954.
- (8) Marchetti, A.; Tinari, N.; Buttitta, F.; Chella, A.; Angeletti, C. A.; Sacco, R.; Mucilli, F.; Ullrich, A.; Iacobelli, S. *Cancer Res.* **2002**, *62*, 2535.
- (9) Kunzli, B. M.; Berberat, P. O.; Zhu, Z. W.; Martignoni, M.; Kleeff, J.; Tempia-Caliera, A. A.; Fukuda, M.; Zimmermann, A.; Friess, H.; Buchler, M. W. *Cancer* **2002**, *94*, 228.
- (10) Fusco, O.; Querzoli, P.; Nenci, I.; Natoli, C.; Brakebush, C.; Ullrich, A.; Iacobelli, S. *Int. J. Cancer* **1998**, *79*, 23.
- (11) Iacobelli, S.; Sismondi, P.; Giai, M.; D'Egidio, M.; Tinari, N.; Amatetti, C.; Di Stefano, P.; Natoli, C. *Br. J. Cancer* **1994**, *69*, 172.
- (12) Sasaki, T.; Brakebusch, C.; Engel, J.; Timpl, R. *EMBO J.* **1998**, *17*, 1606.
- (13) Nonaka, M.; Ma, B. Y.; Imaeda, H.; Kawabe, K.; Kawasaki, N.; Hodohara, K.; Kawasaki, N.; Andoh, A.; Fujiyama, Y.; Kawasaki, T. *J. Biol. Chem.* **2011**, *286*, 22403.
- (14) Shirure, V. S.; Reynolds, N. M.; Burdick, M. M. *PLoS One* **2012**, *7*, e44529.
- (15) Inohara, H.; Akahani, S.; Kohts, K.; Raz, A. *Cancer Res.* **1996**, *56*, 4530.
- (16) Ulmer, T. A.; Keeler, V.; Loh, L.; Chibbar, R.; Torlakovic, E.; Andre, S.; Gabius, H. J.; Laferte, S. *J. Cell. Biochem.* **2006**, *98*, 1351.
- (17) Zhao, Q.; Barclay, M.; Hilken, J.; Guo, X.; Barrow, H.; Rhodes, J. M.; Yu, L. G. *Mol. Cancer* **2010**, *9*, 154.
- (18) Ozaki, Y.; Kontani, K.; Teramoto, K.; Fujita, T.; Tezuka, N.; Sawai, S.; Maeda, T.; Watanabe, H.; Fujino, S.; Asai, T.; Ohkubo, I. *Oncol. Rep.* **2004**, *12*, 1071.
- (19) Mbeunkui, F.; Metge, B. J.; Shevde, L. A.; Pannell, L. K. *J. Proteome Res.* **2007**, *6*, 2993.
- (20) Song, X.; Xia, B.; Stowell, S. R.; Lasanajak, Y.; Smith, D. F.; Cummings, R. D. *Chem. Biol.* **2009**, *16*, 36.
- (21) Stowell, S. R.; Arthur, C. M.; Mehta, P.; Slanina, K. A.; Blixt, O.; Leffler, H.; Smith, D. F.; Cummings, R. D. *J. Biol. Chem.* **2008**, *283*, 10109.
- (22) Hirabayashi, J.; Hashidate, T.; Arata, Y.; Nishi, N.; Nakamura, T.; Hirashima, M.; Urashima, T.; Oka, T.; Futai, M.; Muller, W. E.; Yagi, F.; Kasai, K. *Biochim. Biophys. Acta* **2002**, *1572*, 232.
- (23) Lee, P. L.; Kohler, J. J.; Pfeffer, S. R. *Glycobiology* **2009**, *19*, 655.
- (24) Dennis, J. W.; Nabi, I. R.; Demetriou, M. *Cell* **2009**, *139*, 1229.
- (25) Granovsky, M.; Fata, J.; Pawling, J.; Muller, W. J.; Khokha, R.; Dennis, J. W. *Nat. Med.* **2000**, *6*, 306.
- (26) Ito, N.; Imai, S.; Haga, S.; Nagaïke, C.; Morimura, Y.; Hatake, K. *Histochem. Cell Biol.* **1996**, *106*, 331.
- (27) Srinivasan, N.; Bane, S. M.; Ahire, S. D.; Ingle, A. D.; Kalraiya, R. D. *Glycoconjugate J.* **2009**, *26*, 445.
- (28) Di Virgilio, S.; Glushka, J.; Moremen, K.; Pierce, M. *Glycobiology* **1999**, *9*, 353.
- (29) Wai Wong, C.; Dye, D. E.; Coombe, D. R. *Int. J. Cell Biol.* **2012**, *2012*, 1.